Selective photoinactivation of protein function through environment-sensitive switching of singlet oxygen generation by photosensitizer

Takatoshi Yogo*†, Yasuteru Urano*‡, Akiko Mizushima§, Hisato Sunahara*†, Takanari Inoue*, Kenzo Hirose¶, Masamitsu Iino§, Kazuya Kikuchi‖, and Tetsuo Nagano*†**

*Graduate School of Pharmaceutical Sciences and §Department of Pharmacology, Graduate School of Medicine, University of Tokyo, 7-3-1 Hongo, Bunkyo-ku, Tokyo 113-0033, Japan; †Core Research for Evolutional Science and Technology (CREST) and ‡Precursory Research for Embryonic Science and Technology (PRESTO), Japan Science and Technology Agency, 4-1-8 Honcho Kawaguchi, Saitama 332-0012, Japan; ¶Department of Cell Physiology, Nagoya University Graduate School of Medicine, 65 Tsurumai, Showa, Nagoya, Aichi 466-8550, Japan; and ‖Graduate School of Engineering, Division of Advanced Science and Biotechnology, Osaka University, 2-1 Yamada-oka, Suita, Osaka 565-0871, Japan

Edited by Koji Nakanishi, Columbia University, New York, NY, and accepted by the Editorial Board November 5, 2007 (received for review December 30, 2006)

Chromophore-assisted light inactivation is a promising technique to inactivate selected proteins with high spatial and temporal resolution in living cells, but its use has been limited because of the lack of a methodology to prevent nonspecific photodamage in the cell owing to reactive oxygen species generated by the photosensitizer. Here we present a design strategy for photosensitizers with an environment-sensitive off/on switch for singlet oxygen ($^1O_2$) generation, which is switched on by binding to the target, to improve the specificity of protein photoinactivation. $^1O_2$ generation in the unbound state is quenched by photoinduced electron transfer, whereas $^1O_2$ generation can occur in the hydrophobic environment provided by the target protein, after specific binding. Inositol 1,4,5-trisphosphate receptor, which has been suggested to have a hydrophobic pocket around the ligand binding site, was specifically inactivated by an environment-sensitive photosensitizer-conjugated inositol 1,4,5-trisphosphate receptor ligand without $^1O_2$ generation in the cytosol of the target cells, despite light illumination, demonstrating the potential of environment-sensitive photosensitizers to allow high-resolution control of generation of reactive oxygen species in the cell.

activatable photosensitizer | boron dipyrromethene derivative | electron transfer | inositol 1,4,5-trisphosphate receptor

Chromophore-assisted light inactivation (CALI)(1) is a technique with great potential to inactivate proteins with high spatial and temporal resolution by using an antibody to direct a suitable fluorophore specifically to the protein of interest. Illumination induces local generation of reactive oxygen species (ROS), which react chemically with the adjacent antigen and inactivate it. Although CALI is a powerful technique, its use has been limited by the complexity of the procedures (i.e., the need to deliver a labeled antibody into cells or to use a laser as the light source). Several groups have reported alternative approaches. Genetically targeted CALI is one such method, in which the target protein is tagged with a tetracysteine tag that is recognized by a membrane-permeant biarsenical chromophore (FlAsH) (2, 3), or tagged with GFP (4–6). However, these methods also cause nonspecific damage, owing to the nonspecific binding of the biarsenical chromophore to cysteine-rich proteins (3, 7) in FlAsH-mediated photoinactivation, or to the use of a relatively high-power laser in EGFP-mediated CALI (4, 5). Current implementations of the CALI technique leave much to be desired, and highly specific inactivation of a protein of interest would require a methodology to control ROS generation by the photosensitizer in the cells with high spatial resolution.

We present here an approach for designing photosensitizers with an environment-controlled off/on switch for singlet oxygen ($^1O_2$) generation to improve the specificity of CALI. We have developed environment-sensitive photosensitizers (ESPers), which are activated by recognition of the hydrophobic (low-polarity) environment of the target protein, i.e., recognition of the appropriate environment switches on local generation of $^1O_2$, whereas $^1O_2$ is not generated in the polar cytosolic environment (Fig. 1*a*). The value of ESPers to control tightly the specificity of protein photoinactivation in the CALI technique was demonstrated by applying one of our ESPers for highly specific inactivation of inositol 1,4,5-trisphosphate receptor (IP_3R).

Results

Photoinduced Electron Transfer as a Mechanism to Control Photosensitization. We previously developed small molecule-based CALI for IP_3R by using a conventional photosensitizer (malachite green), and the physiological function of IP_3R was analyzed (8, 9). However, it would be advantageous for further biological applications if an activatable photosensitizer, which generates ROS only when it binds to IP_3R, could be developed. With this in mind, we focused on hydrophobic environment as a putative on-switch for an activatable photosensitizer. Intracellular proteins (e.g., the receptor of interest) usually consist of both hydrophobic and hydrophilic domains, and we considered that a hydrophobic photosensitizer moiety, if it is conjugated to a specific ligand of the target protein by a suitable linker, could be delivered to a hydrophobic domain near the ligand binding site inside the target protein by hydrophobic interaction. In the case of IP_3R, it has been suggested that IP_3R has a hydrophobic pocket around the binding site, based on the finding that IP_3 derivatives bearing a hydrophobic moiety have high binding affinity (10, 11). Thus, photosensitizers that could generate ROS only when they are activated by recognition of the hydrophobic environment around IP_3R should cause little or no nonspecific damage in the cytosol, where the environment is polar (Fig. 1*a*). To realize this concept, we selected photoinduced electron transfer (PeT) as a switch mechanism to control the $^1O_2$ generation of photosensitizers. PeT is a well known mechanism through which the fluorescence of a fluorophore is quenched by electron transfer from the PeT donor to the lowest singlet-excited fluorophore (12, 13). Photosensitization is well known to

Author contributions: Y.U., T.Y., and T.N. designed research; T.Y. performed research; A.M., H.S., T.I., K.H., M.I., and K.K. contributed new reagents/analytic tools; and T.Y., Y.U., and T.N. wrote the paper.

The authors declare no conflict of interest.

This article is a PNAS Direct Submission. K.N. is a guest editor invited by the Editorial Board.

**To whom correspondence should be sent at the * address. E-mail: tlong@mol.f.u-tokyo.ac.jp.

This article contains supporting information online at www.pnas.org/cgi/content/full/0611717105/DC1.

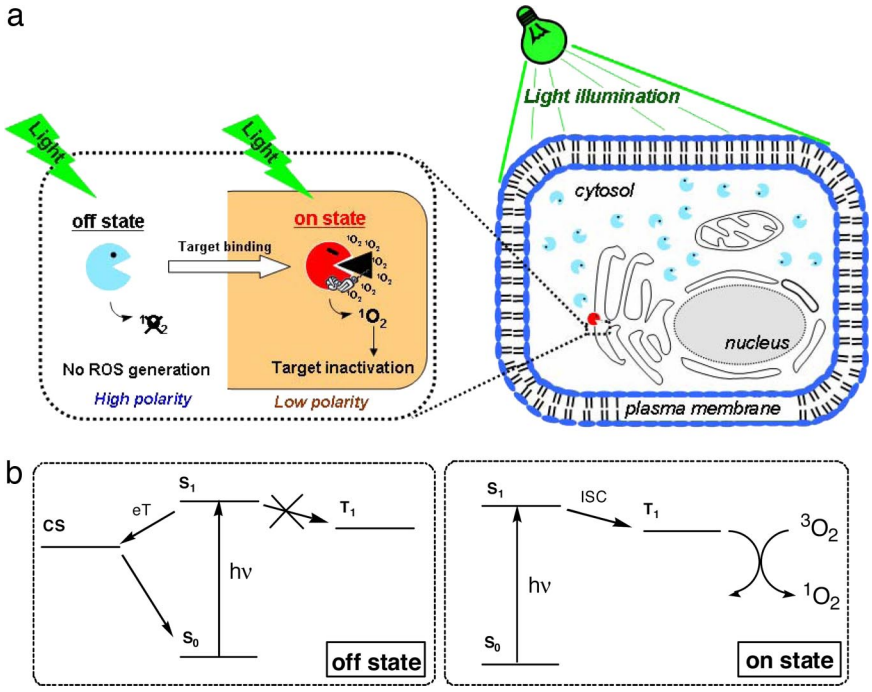

Fig. 1. Photoinduced electron transfer as a mechanism for controlling photosensitization in biological systems. (*a*) Schematic representation of protein photoinactivation by using ESPers. In the cytosolic polar environment, ESPers are in the off state of photosensitization (indicated by light blue) and do not generate $^1O_2$. In the hydrophobic environment of the target, ESPers are in the on state of photosensitization (indicated by red) and generate $^1O_2$, inducing inactivation of the nearby protein of interest. (*b*) Energy diagram of the ESPers. ISC, intersystem crossing; CS, charge separation; eT, electron transfer; S_0, singlet ground state; S_1, lowest singlet excited state; T_1, lowest triplet excited state.

proceed also via the lowest singlet excited state (S_1), so it seemed reasonable that the photosensitization process could be controlled by PeT (Fig. 1*b*). Indeed, our preliminary results showed that $^1O_2$ generation of erythrosin derivatives upon light illumination was efficiently quenched by introducing electron-donating substituents into the benzene moiety (S. Kamakura, Y.U., and T.N., unpublished results). The PeT process is known to depend on the highest occupied molecular orbital (HOMO) energy level of the electron donor and the solvent polarity, so we designed and synthesized a series of photosensitizer derivatives by attaching an electron donor moiety to a photosensitizing chromophore for the specific inactivation of IP_3R in a hydrophobic environment.

Design and Synthesis of a Library of Candidate ESPers. We recently reported development of 4,4-difluoro-2,6-diiodo-1,3,5,7-tetramethyl-4-bora-3a,4a-diaza-*s*-indacene (2I-BDP) as a photosensitizer that generates $^1O_2$ uniformly in various solvents ranging from H_2O to *n*-hexane (14). We hypothesized that introduction of a suitable electron-donor moiety into 2I-BDP would allow the photosensitizing ability to be controlled precisely by means of PeT. To test this principle, we synthesized various 2I-BDP derivatives bearing a substituted benzene moiety (**1a–1f**), in which the use of various substituents (methyl, methoxy, or amino) as electron donors was expected to allow the HOMO energy level to be finely tuned (Fig. 2*a*). These 2I-BDP derivatives have high values of extinction coefficient ($\varepsilon \approx 1 \times 10^5$ $M^{-1}\cdot cm^{-1}$) at ≈530 nm [supporting information (SI) Fig. 5]. We then examined the ability of these 2I-BDP derivatives to generate $^1O_2$ in various solvents, from polar to nonpolar, by observing the disappearance of 1,3-diphenylisobenzofuran (DPBF), which is known to react with $^1O_2$ under light illumination (15) (for detailed experimental procedures, see *SI Materials and Methods*). The relative efficiencies of $^1O_2$ generation (ϕ_Δ) of **1a–1f** in each solvent are summarized in Fig. 2*b*. These 2I-BDP derivatives had almost identical absorbance maximum wavelengths (SI Fig. 5), but the ϕ_Δ of certain 2I-BDP derivatives, i.e., those having an electron donor moiety with high HOMO energy (**1c–1f**), was significantly quenched in polar solvents such as CH_3CN and MeOH, compared with that of **1a** and **1b**, whose benzene moiety has a relatively low HOMO energy. These results suggested that ϕ_Δ of these 2I-BDP derivatives could indeed be controlled by PeT. We then examined the effect of solvent polarity. We have recently developed environment-sensitive fluorescence probes based on the boron dipyrromethene (BODIPY) fluorophore, whose fluorescence properties were shown to be controlled by PeT and by solvent effects on the PeT (see also SI Fig. 6). Because 2I-BDP derivatives are iodinated derivatives of BODIPY, they may behave similarly. Fig. 2*b* shows that ϕ_Δ of **1c–1f** was dependent on the solvent polarity (i.e., dielectric constant, DC). Compounds **1c–1e** were unable to generate $^1O_2$ (i.e., they were in the off state of photosensitization) in solvents more polar than acetone (DC ≈ 20.7), whereas the $^1O_2$-generating ability was restored (i.e., the compounds were in the on state of photosensitization) in solvents less polar than CH_2Cl_2 (DC ≈ 9.14). On the other hand, **1f** was still in the off state in CH_2Cl_2, and was switched on only in solvents less polar than $CHCl_3$ (DC ≈ 4.81), indicating that the threshold for off–on switching of $^1O_2$ generation is dependent on the HOMO energy level of the benzene moiety. These results indicated that appropriately designed 2I-BDP derivatives, having a HOMO energy around −0.17 to −0.19 hartree, could be used as environment-sensitive photosensitizers (ESPers), which would be activated by recognizing a hydrophobic environment, and would generate $^1O_2$ in such an environment, but not in a polar environment. We then examined whether ESPers could be activated by recognizing a hydrophobic environment at the cellular level.

Design of ESPer-Conjugated IP_3 Ligand for Specific Photoinactivation of IP_3R. We next designed and synthesized an ESPer-conjugated IP_3R ligand for photoinactivation of IP_3R and examined whether

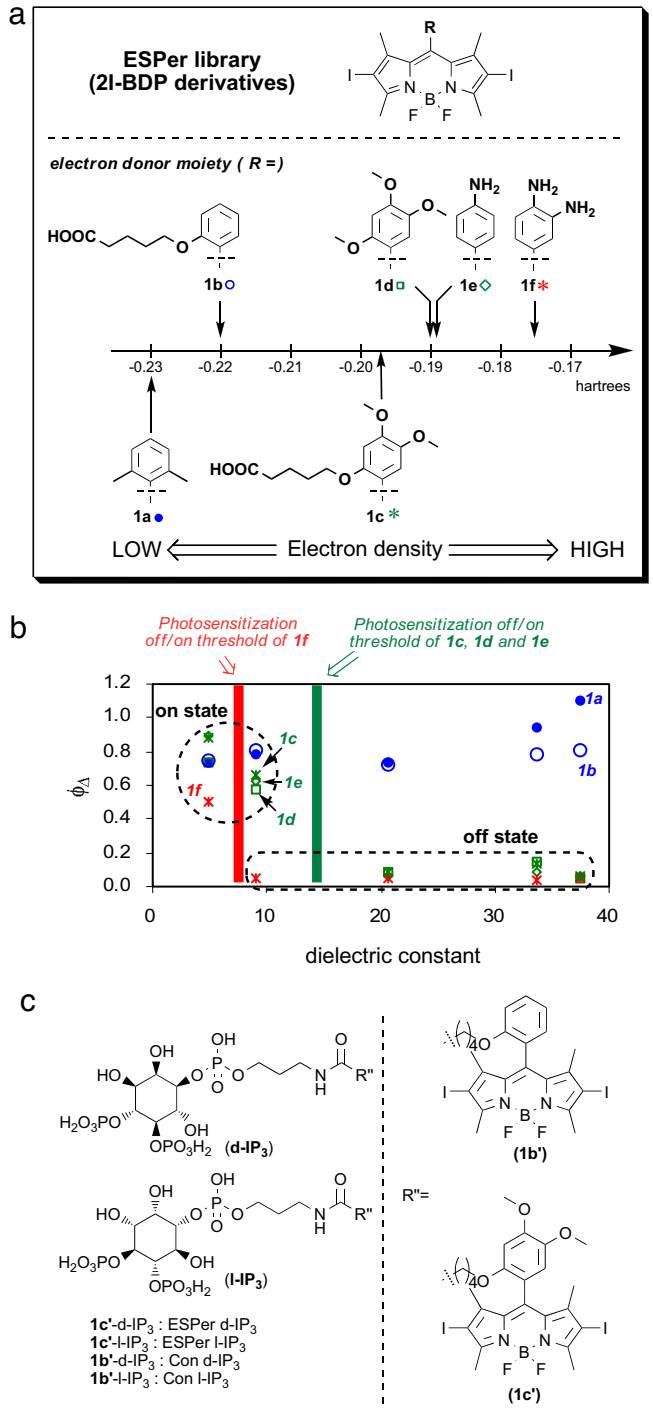

Fig. 2. Development of a library of ESPers making use of the solvent effect on PeT. (*a*) Structures of 2I-BDP derivatives with various benzene moieties. (*b*) Relationship between the relative efficiency of $^1O_2$ generation (ϕ_Δ) of 2I-BDP derivatives (**1a**–**1f**) and the dielectric constant of the solvent. Solvents used in this study were CH_3CN, MeOH, acetone, CH_2Cl_2, and $CHCl_3$, whose dielectric constants are 37.5, 33.6, 20.7, 9.14, and 4.81, respectively. Filled blue circle, **1a**; open blue circle, **1b**; green star, **1c**; open green square, **1d**; open green diamond, **1e**; red star, **1f**. (*c*) Structures of ESPer **1c**-conjugated IP_3 derivatives and control (Con) photosensitizer **1b**-conjugated IP_3 derivatives; d- and l- refer to the D and L absolute configurations of inositol 1,4,5-trisphosphate.

it could generate $^1O_2$ specifically in the vicinity of IP_3R. IP_3R has been suggested to have a hydrophobic pocket around the binding site, which was estimated to be similar in polarity to CH_2Cl_2

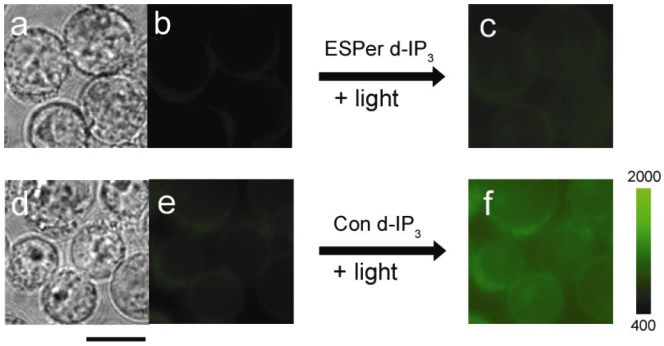

Fig. 3. Imaging of photosensitizer-induced nonspecific cytosolic $^1O_2$ generation in the presence of ESPer d-IP_3, compared with that in the presence of Con d-IP_3, using a fluorescence probe for $^1O_2$ (DMAX-2). Permeabilized DT40 cells (wild type) were loaded with 3 μM ESPer d-IP_3 or Con d-IP_3 and 10 μM DMAX-2, followed by illumination with green light (BP530–550 nm, 1.5 mW/cm^2, 20 sec). Fluorescence images of DMAX-2 were acquired with a fluorescence microscope by excitation with blue light (BA470–490) before and after green light illumination. (*a*–*c*) Single DT40 cells under transmitted light (*a*) and fluorescence image excited with blue light before (*b*) and after (*c*) excitation of ESPer d-IP_3 with green light. (*d*–*f*) Single DT40 cells under transmitted light (*d*) and fluorescence image excited with blue light before (*e*) and after (*f*) excitation of Con d-IP_3 with green light. Color scale on the right is the relative fluorescence intensity. (Scale bar, 10 μm.)

(DC $\approx$ 9.14) by the use of environment-sensitive fluorescence probes (*SI Materials and Methods* and SI Fig. 6). Thus, we considered that **1c** and **1d** (Fig. 2*a*), which have a trimethoxybenzene moiety, might be suitable ESPers to recognize the environment around IP_3R. We synthesized an IP_3 derivative bearing **1c** (Fig. 2*c*). As a control (Con) compound, we also synthesized an IP_3 derivative bearing **1b**, whose off/on switch for $^1O_2$ generation is constitutively on (Fig. 2 *a* and *b*), regardless of the environment. d-IP_3 derivatives were designed as IP_3 ligands that bind to IP_3R, and l-IP_3 derivatives (optical isomers of d-IP_3), which are expected to have the same photochemical properties as those of d-IP_3 derivatives, although with much weaker agonistic effects on IP_3R (8), were also synthesized (Fig. 2*c*). These photosensitizer-conjugated d-IP_3 derivatives induced Ca^{2+} release via IP_3R in a dose–response manner with an EC_{50} of 3 μM for both ESPer d-IP_3 and Con d-IP_3, whereas the photosensitizer-conjugated l-IP_3 derivatives had almost no Ca^{2+} release activity (SI Fig. 7).

Imaging of Photosensitizer-Induced Nonspecific Damage Caused by ESPer d-IP_3 and Con d-IP_3 in the Cytosolic Polar Environment. We examined whether ESPer d-IP_3 outside the hydrophobic IP_3R environment (e.g., in the cytosolic polar environment) indeed lacked $^1O_2$-generating ability (off state of photosensitization) despite light illumination, whether $^1O_2$-generating ability was recovered in the vicinity of IP_3R (on state of photosensitization), and whether IP_3R could be inactivated by the $^1O_2$ generated (as illustrated in Fig. 1*a*). We first studied whether ESPer d-IP_3 generated $^1O_2$ in the cytosol in the cells by fluorescence imaging of $^1O_2$ generation with a fluorescent probe for $^1O_2$ (DMAX-2) (16) in permeabilized DT40 cells (wild type). Permeabilized DT40 cells were loaded with 3 μM ESPer d-IP_3 (or Con d-IP_3) and 10 μM DMAX-2, followed by illumination with green light (BP530–550 nm, 1.5 mW/cm^2, 20 sec) to excite the photosensitizer. ESPer d-IP_3-loaded cells showed little, if any, fluorescence increase of DMAX-2 upon light illumination (Fig. 3 *a*–*c*). On the other hand, Con d-IP_3-loaded cells showed a marked fluorescence increase of DMAX-2 in cytosol (Fig. 3 *d*–*e*), owing to nonspecific $^1O_2$ generation in the polar cytosolic environment, as shown in Fig. 2*b*. The fluorescence increase induced by DMAX-2 in Con d-IP_3-loaded cells was inhibited by adding a $^1O_2$ quencher

(20 mM NaN_3) (SI Fig. 8). These results clearly demonstrate that nonspecific photosensitizer-induced $^1O_2$ generation outside the environment of interest can be significantly reduced by designing a suitable photosensitizer with an off/on switch for $^1O_2$ generation. We next investigated whether ESPer-IP_3 could specifically acquire $^1O_2$-generating ability in the hydrophobic environment in the vicinity of IP_3R.

ESPer-Mediated Photoinactivation of IP_3R in Cells. We examined whether ESPer d-IP_3, which has been shown not to generate $^1O_2$ in cytosol (Fig. 3), could induce IP_3R inactivation through $^1O_2$ generation after recognition of the hydrophobic environment of IP_3R in DT40 cells (wild type). DT40 cells were loaded with Furaptra acetoxymethyl ester (AM) as a Ca^{2+} indicator, then permeabilized with β-escin to retain the probe only in the endoplasmic reticulum (ER), enabling us to continuously monitor luminal Ca^{2+} concentration ($[Ca^{2+}]l$) within the store (17). An increase in $[Ca^{2+}]l$ was observed upon activation of sarco/endoplasmic reticulum Ca^{2+}-ATPase (SERCA) with application of both Ca^{2+} and MgATP, followed by a decrease upon addition of IP_3. First, by monitoring $[Ca^{2+}]l$ within permeabilized DT40 cells, we measured the IP_3-induced Ca^{2+} release (IICR) rate at 10 μM IP_3. The cells were then illuminated for 5 sec with green light (535 ± 25 nm, 20 mW) in the presence of 2 μM test photosensitizer. The photosensitizer was washed out, and the IICR rate was measured again and compared with that at pretreatment. A considerable decrease in the IICR rate was observed (IICR rate pretreatment = 0.194 ± 0.0084 sec^{-1}, IICR rate after treatment = 0.093 ± 0.0071 sec^{-1}; Fig. 4 *a* and *b*) after light illumination in the presence of ESPer d-IP_3. The extent of this decrease of the IICR rate owing to ESPer d-IP_3-mediated photoinactivation of IP_3R was similar to that in the case of Con d-IP_3-mediated photoinactivation (Fig. 4*b*). On the other hand, the optical isomers (i.e., ESPer l-IP_3 and Con l-IP_3) did not cause receptor inactivation upon light illumination (Fig. 4 *a* and *b*), indicating that the inactivation of IP_3R required the binding of ESPer d-IP_3 to the receptor. Furthermore, the photoinactivation caused by ESPer d-IP_3 or Con d-IP_3 was inhibited by adding a $^1O_2$ quencher (20 mM NaN_3) to the intracellular solution (Fig. 4*b*), suggesting that the inactivation of IP_3R by ESPer d-IP_3 was mediated by $^1O_2$. The activity of SERCA protein, which is colocalized with IP_3R on the ER membrane (18), was not affected by ESPer d-IP_3-mediated photoinactivation (SI Fig. 9), suggesting that little or no nonspecific damage to nontargeted protein present on the same intracellular organelle as IP_3R was induced by light illumination. These results demonstrated that ESPer d-IP_3 could bind to IP_3R, where it recognized the hydrophobic environment, and was activated to generate $^1O_2$, resulting in highly specific receptor inactivation.

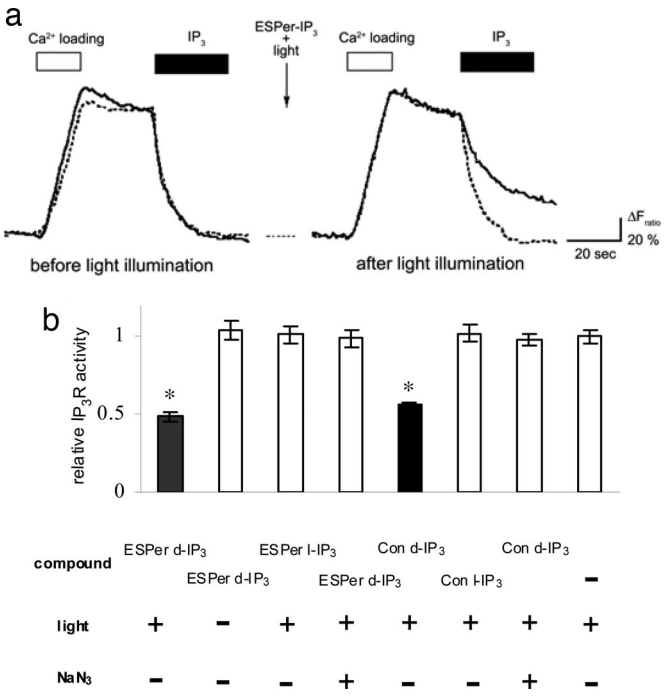

Fig. 4. ESPer-mediated light inactivation of the target protein in a hydrophobic environment. (*a*) ESPer d-IP_3-mediated light inactivation of IP_3R. After measurement of the IICR rate at 10 μM IP_3, permeabilized DT40 cells (wild type) were pretreated with 2 μM ESPer d-IP_3 (solid line) or 2 μM ESPer l-IP_3 (dotted line) followed by light illumination at 530 nm (20 mW/cm^2) for 5 sec. After the irradiation and immediate washout of the ESPer d- or l-IP_3-containing solution, the IICR rate at 10 μM IP_3 of the illuminated cells was measured. Traces show Ca^{2+} responses in a single DT40 cell. Note that there is a considerable difference between the IICR rates before and after the treatment. (*b*) The IICR rate after 5-sec light illumination with or without test compound, light illumination, and 20 mM NaN_3 was normalized to that before illumination. A significant difference was found when the relative Ca^{2+} release rate of the illuminated cells loaded with ESPer d-IP_3 or Con d-IP_3 in the absence of NaN_3 (filled columns) was compared with that of cells under other conditions (open columns) [*, $P < 0.0001$, Fisher's probable least-squares difference (PLSD) test]. The number of images of analyzed cells was 25, acquired in three independent experiments. Error bars represent SEM.

Discussion

We have developed an environment-sensitive photosensitizer, which is activated upon recognizing the hydrophobic environment of a protein of interest and generates $^1O_2$ only within this environment to achieve highly specific photoinactivation based on the CALI technique. We designed an ESPer-conjugated IP_3R ligand (ESPer d-IP_3), which would be activated in the range of polarity of CH_2Cl_2 (Fig. 2). ESPer d-IP_3 did not generate $^1O_2$ outside the IP_3R environment even under light illumination (Fig. 3), but acquired $^1O_2$-generating ability in the hydrophobic environment in the vicinity of IP_3R (Fig. 4). We now plan to apply ESPer d-IP_3 to neuronal cells to examine the specificity of ESPer d-IP_3 in intact cells and study physiological functions of IP_3R. Such an activatable photosensitizer permits highly regiospecific generation of $^1O_2$ at the target protein, with little or no nonspecific phototoxicity elsewhere in the cell. So far, the use of photosensitizers has required great care to avoid nonspecific damage, and the specificity of the photosensitizing effect has often been dependent on the precise localization of photosensitizers in the cell or whole body (19), which cannot be easily predicted and requires much experimental effort to determine. On the other hand, our design approach to ESPers enables us to predict the efficiency of $^1O_2$ generation by calculation of the HOMO energy level of the electron donor moiety, and we could prepare a series of photosensitizers with off/on switches operating at various cellular properties, such as pH and specific enzyme. Furthermore, ESPers could be excited by using conventional equipment such as the xenon light of a fluorescence microscope. Of course, when designing a novel activatable photosensitizer for the inactivation of another target protein based on the above-mentioned approach, specificity should be thoroughly examined; however, our rational design strategy should expand the applicability of photosensitizers in biological research, as well as clinical applications, by allowing tight control of the regiospecificity of photosensitization through switching on $^1O_2$-generating ability only after binding of the photosensitizer to the designated target.

Materials and Methods

Chemical Synthesis. For detailed synthetic procedures, characterization of products, and photochemical properties of BODIPY derivatives, see *SI Materials and Methods* and SI Schemes 1–5.

Fluorescence Imaging. Fluorescence images were acquired with an inverted microscope (IX71; Olympus), equipped with a cooled CCD camera (Cool Snap HQ; Roper Scientific) and a xenon lamp (AH2-RX; Olympus). The whole system was controlled with MetaFluor 6.1 software (Universal Imaging). For imaging $^1O_2$ generation by DMAX-2 (for details of the characteristics of DMAX-2, see also SI Fig. 10), DT40 cells (wild type) attached to the coverslips were permeabilized with 60 μM β-escin for 1–2 min. Cells were loaded with 3 μM Con d-IP$_3$ or ESPer d-IP$_3$ and 10 μM DMAX-2, and fluorescence images (excitation filter, BA470–490; dichroic mirror, DM505; emission filter, BA510–550; Olympus) were acquired immediately after illumination with green light (BP530–550 nm, 1.5 mW/cm^2, 20 sec).

Luminal Ca^{2+} Imaging of DT40 Cells. Ca^{2+} imaging of DT40 cells was performed as described previously (17) (see also *SI Materials and Methods*). Briefly, DT40 cells (wild type) were loaded with Furaptra AM, a membrane-permeant, low-affinity Ca^{2+} indicator, which enters both the cytosol and organelles. Furaptra-loaded cells were then permeabilized with β-escin so that Furaptra was retained only in the ER, enabling us to continuously monitor luminal Ca^{2+} concentration ([Ca^{2+}]l) within the store. An increase in [Ca^{2+}]l was observed upon activation of sarco/endoplasmic reticulum Ca^{2+}-ATPase (SERCA) with application of both Ca^{2+} and MgATP, followed by a decrease upon addition of IP$_3$. This Ca^{2+} loading and release procedure can be repeated reproducibly in the same cells, and the rate constant of IP$_3$-induced Ca^{2+} release (IICR) was used as an index of IP$_3$R activity.

Light Illumination for Photoinactivation of IP$_3$R. First, by monitoring [Ca^{2+}]l within permeabilized DT40 cells, we measured the IICR rate at 10 μM IP$_3$. The cells were then illuminated for 5 sec in the presence of 2 μM test photosensitizer with a xenon lamp (AH2-RX), which was filtered to $\approx$535 $\pm$ 25 nm by an excitation filter (HQ535/50; Chroma Technology) through the objective lens under the fluorescence microscope. The photosensitizer was washed out, and the IICR rate was measured again and compared with the pretreatment value.

ACKNOWLEDGMENTS. This study was supported by a grant for Precursory Research for Embryonic Sciences and Technology from the Japan Science and Technology Agency, Research Grants 16651106 and 16689002 from the Ministry of Education, Culture, Sports, Science and Technology of the Japanese Government, and a grant from the Kato Memorial Bioscience Foundation to Y.U.

1. Jay D-G (1988) *Proc Natl Acad Sci USA* 85:5454–5458.
2. Marek K-W, Davis G-W (2002) *Neuron* 36:805–813.
3. Tour O, Meijer R-M, Zacharias D-A, Adams S-R, Tsien R-Y (2003) *Nat Biotechnol* 21:1505–1508.
4. Rajfur Z, Roy P, Otey C, Romer L, Jacobson K (2002) *Nat Cell Biol* 4:286–293.
5. Tanabe T, Oyamada M, Fujita K, Dai P, Tanaka H, Takamatsu T (2005) *Nat Methods* 2:503–505.
6. Bulina M-E, Chudakov D-M, Britanova O-V, Yanushevich Y-G, Staroverov D-B, Chepurnykh T-V, Merzlyak E-M, Shkrob M-A, Lukyanov S, Lukyanov, K-A (2006) *Nat Biotechnol* 24:95–99.
7. Stroffekova K, Proenza C, Beam K-G (2001) *Pflügers Arch* 442:859–866.
8. Inoue T, Kikuchi K, Hirose K, Iino M, Nagano T (2003) *Chem Biol* 10:503–509.
9. Yogo T, Kikuchi K, Inoue T, Hirose K, Iino M, Nagano T (2004) *Chem Biol* 11:1053–1058.
10. Inoue T, Kikuchi K, Hirose K, Iino M, Nagano T (1999) *Bioorg Med Chem Lett* 9:1697–1702.
11. Nakanishi W, Kikuchi K, Inoue T, Hirose K, Iino M, Nagano T (2002) *Bioorg Med Chem Lett* 12:911–913.
12. Miura T, Urano Y, Tanaka K, Nagano T, Ohkubo K, Fukuzumi S (2003) *J Am Chem Soc* 125: 8666–8671.
13. Urano Y, Kamiya M, Kanda K, Ueno T, Hirose K, Nagano T (2005) *J Am Chem Soc* 127:4888–4894.
14. Yogo T, Urano Y, Ishitsuka Y, Maniwa F, Nagano T (2005) *J Am Chem Soc* 127:12162–12163.
15. Lissi E-A, Encinas M-V, Lemp E, Rubio M-A (1993) *Chem Rev* 93:699–723.
16. Tanaka K, Miura T, Umezawa N, Urano Y, Kikuchi K, Higuchi T, Nagano T (2001) *J Am Chem Soc* 123:2530–2536.
17. Miyakawa T, Maeda A, Yamazawa T, Hirose K, Kurosaki T, Iino M (1999) *EMBO J* 18:1303–1308.
18. Hirose K, Iino M (1994) *Nature* 372:791–794.
19. Jori G (1996) *J Photochem Photobiol B* 36:87–93.